Propagation pathways from meteorological to agricultural drought in different climatic basins in Iran

Mehdi Mohammadi Ghaleni[1,2*], Saeed Sharafi[3] and Mahmood Sadat-Noori[4]

[1] Assistant Professor, Department of Water Science and Engineering, Arak University, Arak, Iran

[2] Research Institute for Water Science and Engineering, Arak University, Arak, Iran.

[*] The first author, Mehdi Mohammadi Ghaleni is corresponding author, email address: m-mohammadighaleni@araku.ac.ir

[3] Assistant Professor, Department of Environment Science and Engineering, Arak University, Arak, Iran. Email address: s-sharafi@araku.ac.ir

[4] College of Science and Engineering, James Cook University, Townsville, QLD 4814, Australia. Email address: mahmood.sadatnoori@jcu.edu.au

Abstract

The propagation of meteorological drought (MD) to agricultural drought (AD) is influenced by various factors, particularly the climate type. This research examined the characteristics of drought propagation, encompassing propagation rates, lag time, and response time, from MD to AD within the context of Iran's diverse climate conditions. This was accomplished using three crucial meteorological and agricultural drought indices, namely the Standardized Precipitation Evapotranspiration Index (SPEI), Standardized Precipitation Index (SPI), and Standardized Soil Moisture Index. The research data included in-situ and ERA5 datasets from 30 basins (catchments) across Iran in the 1979–2021 period. Based on reports from the Global Drought Observatory, the three most prominent MD events were identified in 1999–2002, 2008–2009, and 2017–2019. The correlation coefficients between MD and AD indices across various timescales, in climates ranging from hyper-arid to humid, exhibited a decline from 0.75 to 0.44. The response time, varying between 2.42 to 6.63 months, was determined by the strong correlation between SPI (or SPEI) and SSI1 (or SSI2) within the studied basins. Furthermore, the lag time, which was affected by the onset of MD and AD events, fluctuated between 2 to 6 months in hyper-arid and arid basins, revealing a 1–3 month variation compared to humid basins. The findings on propagation rates highlighted heightened sensitivity or response from meteorological to agricultural drought in humid climates, as opposed to hyper-arid climates. In light of these outcomes, comprehending the transition from MD to AD holds substantial significance for predicting, issuing early warnings, and fortifying preparedness in managing drought risks.

Keywords: agricultural drought, controlling factors, drought propagation, Iran, response time

1. Introduction

Aridity represents a consistent aspect of climate, determined by enduring climatic patterns across a region. In contrast, drought represents a temporary departure from typical weather patterns and can occur in diverse climates (Karamouz et al., 2012; Araghi et al., 2018). Drought, as a recurring natural event that results from inadequate water supply to meet demands, gives rise to agricultural drought (AD), with significant repercussions for both the environment and people's livelihoods. Interrelated drought types, with meteorological drought (MD) as the root cause, have a substantial impact on agriculture, particularly in semi-arid and arid climates. For instance, in Iran—which is situated in a semi-arid zone heavily reliant on precipitation for agricultural output— agriculture is one of the most vulnerable economic sectors (Vogt et al., 2018). Agricultural drought, triggered by deficient precipitation, leads to soil moisture deficits adversely affecting crop yield and plant growth. Drought propagation closely correlates with changes in the features of different drought types (e.g., agricultural, meteorological, socioeconomic, and hydrological) (Vicente-Serrano et al., 2010b). Previous studies have investigated drought propagation, notably the transition from MD to AD, as well as hydrological drought (Huang et al., 2017; Xu et al., 2019; Zhou et al., 2019, 2021; Sattar et al., 2020), and groundwater drought (Han et al., 2019, 2021). Evidence suggests that the transition from MD to AD depends on soil moisture responsiveness to regional precipitation variations (Singh et al., 2021; Afshar et al., 2022).

Various indices are utilized in the literature as agricultural drought indices (ADIs) to investigate drought propagation. Notable examples include the standardized soil moisture index (SSI), soil moisture percentile (SMP), and soil water deficit index (SWDI) (Sheffield et al., 2004; Bae et al., 2019; Behrang Manesh et al., 2019; Gibson et al., 2020; Zhou et al., 2021).

Behrang Manesh et al. (2019) examined the relationship between AD and MD by employing meteorological and agricultural indices across various Iranian regions with differing climates from 2000 to 2017. Their research highlighted a strong correlation and the influence of slope between the 12-month Standardized Precipitation-Evapotranspiration Index (SPEI) and the Vegetation Health Index (VHI) during arid conditions in June. Similarly, Zhu et al. (2021) investigated the potential for drought propagation from MD to soil moisture using SSI and SPEI. Their findings indicated that the duration of AD typically exceeds that of MD in most regions worldwide.

Dai et al. (2022) focused on the Wei River basin in western China in terms of the transition time from MD to AD. They identified shorter propagation times during autumn (3 months) and summer (4.5 months) compared to winter (5 months) and spring (6.7 months) across the entire basin. Furthermore, the propagation time varied from 2 to 8 months among the three sub-regions. Cai et al. (2021) assessed the effects and contributions of MD on AD in different Northwest China climates, utilizing a combination of SPEI and VCI. They found that the primary determiners (76.71%) of AD changes in grasslands were climatic factors.

Um et al. (2022) analyzed drought propagation using several indices in China's Yangtze River basin, estimating shorter propagation periods of 1–2 months for MD to hydrological compared to 1–7 months for MD to agricultural droughts. Weng et al. (2023) employed a 3D method for identifying clusters to detect MD and vegetation drought events and their features across China from 1982 to 2018. They found that vegetation had a complicated response to drought following the mixed effects of moisture and heat stress across various climates and vegetation classes in every region.

Despite substantial advancements in drought propagation research, gaps persist in understanding various aspects of this process. Hence, it is vital to gain a better understanding of

this phenomenon, which can help with the management of water resources under diverse climates. While existing studies have focused on MD propagation to hydrological drought, there has been scant focus on MD to agricultural drought. Additionally, the literature has not accounted for the effect of climate type, as a controlling factor in determining propagation properties. This study aims to evaluate drought propagation, including response time scales, lag time, and propagation rates, from MD to AD in various climate types. Using Iran, known for its diverse climates, as a case study, this study builds upon previous research by investigating drought propagation in Iran's basins to: (1) determine propagation time (i.e., response time scale) and lag time from meteorological to agricultural drought; (2) reveal propagation rates based on drought properties, including event count, frequency, duration, and intensity; and (3) explore the effects of climatic classes on drought propagation properties based on the various climates of the study area.

2. Materials and methods

2.1. Study area

The study area, Iran, is situated between the latitudes of 25°–40° N and longitudes 44°–63° E (Fig. 1). Being the second-biggest country in the Middle East and the seventeenth-biggest in the world, it spans 1,648,195 km^2 in size and boasts a population of approximately 82 million (Bazrafshan and Cheraghalizadeh 2021; Rezaei 2021). Iran's topographical extremes include a depth of 29 meters below sea level (southern coast of the Caspian Sea) and a height of 5,597 meters above mean sea level (Mount Damavand) (Fig. 1a) (Bazrafshan and Cheraghalizadeh, 2021). The mean annual precipitation (P) during the period of 1987–2019 was 357 mm, exhibiting a substantial variation between the lowest (52 mm y^{-1}) and highest (1,692 mm y^{-1}) levels, amounting to 1,640 mm (Fig. 1b) (Madani, 2014; Moshir Panahi et al., 2021). Utilizing the FAO_{56} Penman-

Monteith (PMF_{56}) equation, the regional Potential Evapotranspiration (PET) for the study area was calculated, revealing an approximate mean PET of 4239 mm y^{-1}, which is indicative of the diverse climate from the southern coast of the Caspian Sea to the southeast parts of Iran (Fig. 1c) (Sharafi and Ghaleni, 2022).

The aridity index (AI) for the study area was derived from the ratio of mean annual P to mean annual PET (AI=P/PET). The AI facilitated the categorization of basins (Fig. 1d) into distinct aridity levels, including Hyper-arid (AI ≤0.03), Arid (0.03 < AI ≤ 0.2), Semiarid (0.2 < AI ≤ 0.75), and humid (AI > 0.75) zones (Unesco, 1979; Tsiros et al., 2020).

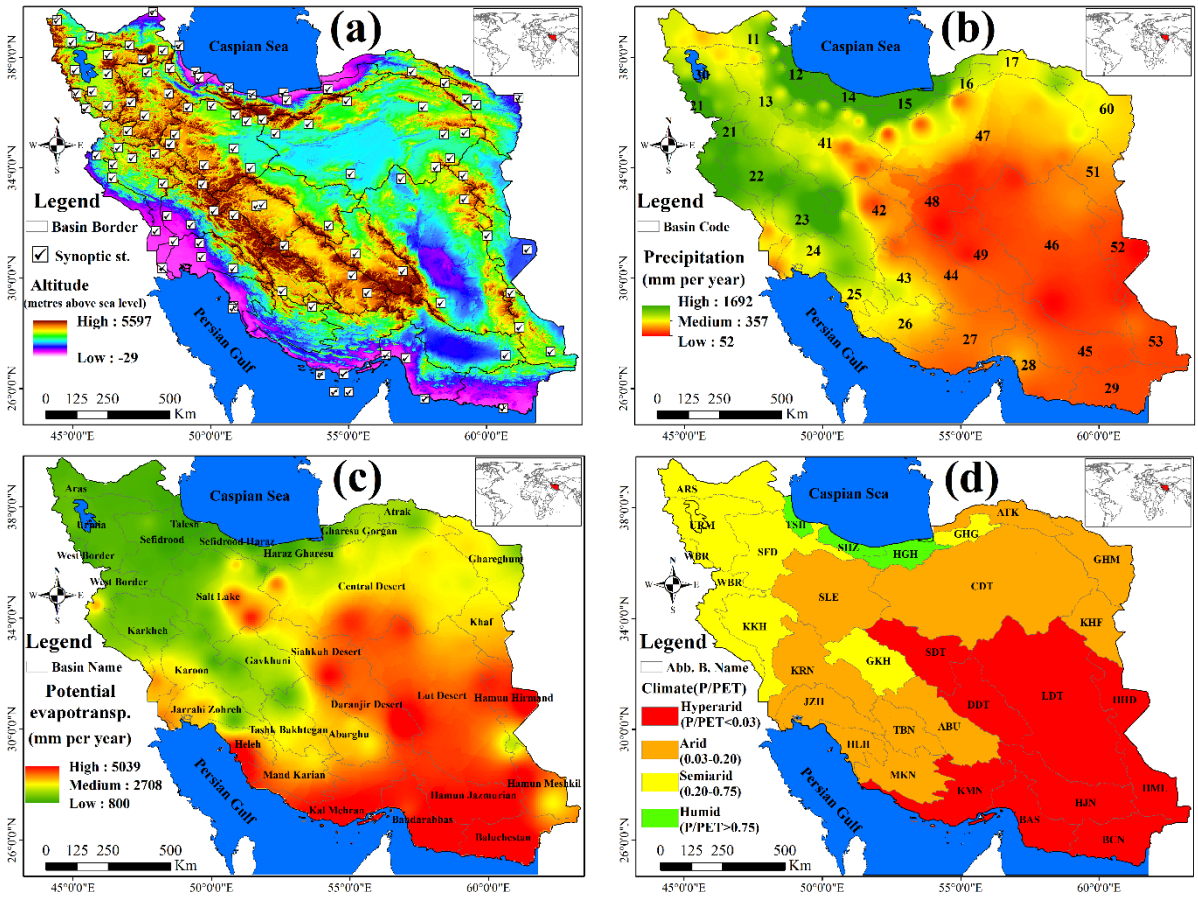

Fig.1. (a) Altitude and location of 100 synoptic stations and borders within 30 basins; (b) Precipitation; (c) Potential Evapotranspiration; (d) Climate classification zones based on the aridity index.

123 *2.2. Dataset*

124 Iran has 30 main hydrological basins, out of which 9 (37% area), 11 (42% area), 7 (18% area),
125 and 3 (2% area) have Hyper-arid (HA), Arid (AR), Semiarid (SA), and Humid (HU) climates,
126 respectively (Fig. 1 d). The characteristics of these 30 basins are presented in Table 1.

127 **Table 1. Characteristics of basins in the present study.**

Row	Basin code	Name	Abb	Area $10^3 km^2$	T_{min} (^OC)	T_{max} (^OC)	P (mm y^{-1})	PET (mm y^{-1})	AI	Climate
1	48	Siahkuh Desert	SDT	48.60	13.2	27.2	59	3514	0.02	Hyper-arid (37% of area)
2	29	Baluchestan	BCN	48.52	23.3	29.5	118	4721	0.03	
3	52	Hamun Hirmand	HHD	33.59	13.1	28.2	82	3053	0.03	
4	49	Daranjir Desert	DDT	50.74	8.8	26.2	98	3503	0.03	
5	45	Hamun Jazmurian	HJN	69.37	20.0	34.2	109	3563	0.03	
6	27	Kal Mehran	KMN	62.90	24.1	31.0	131	4066	0.03	
7	46	Lut Desert	LDT	206.35	14.4	28.0	107	3072	0.03	
8	28	Bandarabbas	BAS	44.79	22.5	32.1	168	3905	0.03	
9	53	Hamun Meshkil	HML	36.51	13.8	28.8	130	2951	0.03	
10	25	Heleh	HLH	21.31	21.3	29.4	257	4068	0.06	Arid (42% of area)
11	51	Khaf	KHF	33.09	6.9	22.7	166	2406	0.07	
12	47	Central Desert	CDT	226.53	11.5	24.1	171	2422	0.07	
13	44	Abarghu	ABU	57.13	7.7	23.8	141	1946	0.07	
14	26	Mand Karian	MKN	47.80	10.5	28.1	281	2319	0.12	
15	60	Ghareghum	GHM	44.30	9.2	22.6	263	2048	0.13	
16	43	Tashk Bakhtegan	TBN	31.45	10.8	26.3	321	2248	0.14	
17	23	Karoon	KRN	66.68	13.8	28.5	314	2108	0.15	
18	41	Salt Lake	SLE	92.88	7.8	21.2	286	1814	0.16	
19	24	Jarrahi Zohreh	JZH	40.82	17.9	32.5	331	2001	0.17	
20	17	Atrak	ATK	26.40	6.5	19.8	332	1874	0.18	
21	11	Aras	ARS	39.78	6.7	18.3	276	1146	0.24	Semiarid (18% of area)
22	30	Urmia	URM	51.76	5.5	18.7	321	1221	0.26	
23	22	Karkheh	KKH	51.91	8.5	24.6	432	1521	0.28	
24	13	Sefidrood	SFD	59.19	5.0	17.8	326	1133	0.29	
25	42	Gavkhuni	GKH	41.55	6.4	21.6	533	1595	0.33	
26	21	West Border	WBR	39.30	8.6	21.2	604	1478	0.41	
27	16	Gharesu Gorgan	GHG	12.99	12.5	23.3	529	959	0.55	
28	15	Haraz Gharesu	HGH	18.77	13.5	21.6	823	897	0.92	Humid (2% of area)
29	14	Sefidrood Haraz	SHZ	10.89	13.4	19.9	1274	868	1.47	
30	12	Talesh	TSH	7.04	12.9	19.7	1474	883	1.67	

128 Note: Basin codes are based on those of Iran's Ministry of Energy. Units of Area, T_{min} and T_{max}, P and PET are 10^3 Km^2, ^oC, mm
129 $year^{-1,}$ and mm $year^{-1}$. AI (Aridity index=P/PET) was calculated based on Unesco (1979).

130

131 This study used three datasets including ground-based In-situ observations (synoptic stations),
132 gauge-based data (CRU TS4.05), and reanalysis products (ERA5) (a summary of the datasets can
133 be seen in Table 1). The daily meteorological variables including P, min and max air temperature
134 (T_{min} and T_{max}), sunshine duration (S), relative humidity (RH), and wind speed (U2) for the period
135 1987–2019 were collected for the 100 synoptic stations from Iranian Meteorological Organization
136 (IRIMO) (Fig. 1a). Daily PET was calculated through FAO56 Penman-Monteith (PMF56)
137 equation (Allen et al., 2006) using measured meteorological variables in these synoptic stations.
138 The characteristics of global gridded products are presented in Table 2.

139 **Table 2. Characteristics of global product datasets.**

Data type	Sources	Resolution		Coverage		Variables	website	References
		Spatial	Temporal	Spatial	Temporal			
In-situ observations	Synoptic stations	Point (100 stations)	daily	Iran	1987-2019	P, T_{min}, T_{max}, RH, S, U_2 and PET_{PMF56}	https://www.irimo.ir/eng/index.php	IR of Iranian Meteorological Organization (IRIMO)
Gauge-based	CRU TS4.05	0.5°×0.5° (624 grids)	monthly	Iran	1901-2020	P, T_{mean}, and PET	https://ceda-wps-ui.ceda.ac.uk/	(Harris et al., 2020)
Reanalysis-based	ERA 5	0.25°×0.25° (2496 grids)	monthly	Iran	1979-2021	SM1-4	https://cds.climate.copernicus.eu/	(Hersbach et al., 2020)

140

141 The gridded Climatic Research Unit Time-series version 4.05 (CRU TS4.05) dataset provides
142 high-resolution (0.5×0.5 degree) grids of monthly ground-based observations over the period
143 1901–2020 (http://www.cru.uea.ac.uk/). A complete report of CRU TS datasets can be found in
144 (Harris et al., 2020). In this study, three monthly variables from CRU TS4.05 datasets including
145 mean temperature (T_{mean}), P, and PET were used with 0.5°×0.5° resolution grids in the 1901–2020
146 period across Iran (Table 2).

147 ERA5 is the latest high-resolution reanalysis product of the Copernicus Climate Change Service
148 at the European Centre for Medium-Range Weather Forecasts, with a spatial resolution of
149 $0.1^{o}\times0.1^{o}$ and a temporal resolution of 1 month covering the period from 1950 to present
150 (https://www.ecmwf.int/en/forecasts/datasets/reanalysis-datasets/era5). Details of ERA5 datasets
151 can be found in Hersbach et al. (2020).

152 ERA5 datasets have been widely used in meteorology, hydrology, ecology, and other research
153 fields (Cai et al., 2021; Huang et al., 2021a; Moshir Panahi et al., 2021; Saemian et al., 2021;
154 Zhang et al., 2021a). Four monthly variables from ERA5—including T_{mean}, total precipitation
155 (TP), PET, and soil moisture (SM)—were used in this study for two layers (layer 1 = 0-7 cm (SM1)
156 and layer 2 = 7-28 cm (SM2)), with a $0.25^{o}\times0.25^{o}$ resolution for the period 1979–2021 (Table 2).

157 Previous research was used to ensure that the gridded climate datasets for CRU (Ababaei, 2020;
158 Collins et al., 2021) and ERA5 (Araghi et al., 2021, 2022; Anvari and Moghaddasi, 2023) are
159 reliable. In addition, the validity of these gridded datasets was affirmed within the study area
160 (i.e., Iran).
161
162 *2.3.Drought identification*
163 *2.3.1. Drought properties*
164 Here, two meteorological drought indices (MDIs), viz., SPI (McKee et al., 1993; McKee, 1995)
165 and SPEI (Vicente-Serrano et al., 2010a), and two ADIs, including SSI1 and SSI2 (Sheffield et
166 al., 2004; Hao and AghaKouchak, 2014), were used to assess drought propagation from MD to
167 AD in 30 basins (Table 1) during 1979–2020. These indices (i.e. SPI, SPEI, SSI1, and SSI2) were
168 calculated in multi-time scales of 1-, 3-, 6-, 9-, 12-, 18-, 24-, and 48-months. Figure 2 illustrates a

169 schematic representation of the features and characteristics of drought events examined in the
170 study.

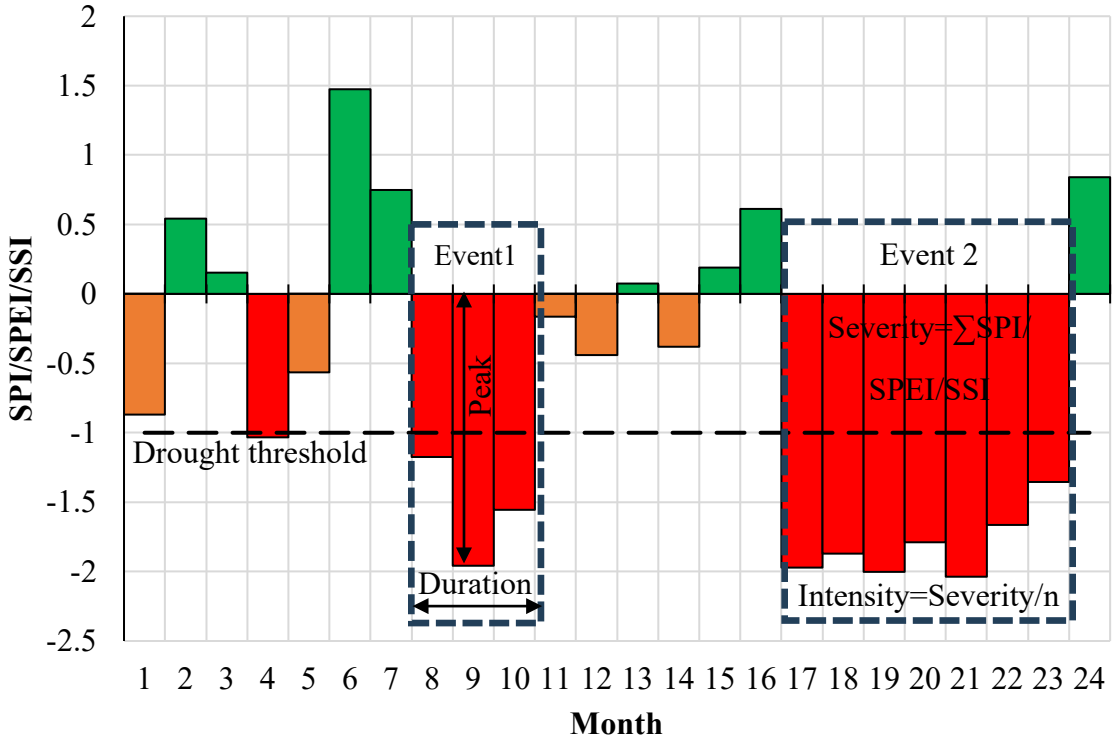

Fig 2. The features of drought events and characteristics

171

172 The value -1 is generally seen as the threshold for determining that a drought has occurred
173 (Haile et al., 2020a). This research considered an event as drought (NDE = number of drought
174 events) when the values of the four drought indices were below -1 for over three successive months
175 (Liu et al., 2016; Haile et al., 2020b). Next, each drought event's features—frequency (DF),
176 duration (DD), and intensity (DI)—were calculated. Drought duration (DD) was determined
177 through Equation (1) (Xu et al., 2019):

$$DD = \frac{\sum_{i=1}^{n} d_i}{n} \qquad (1)$$

where d_i is the duration of the i^{th} drought event and n is the total number of drought events recorded by a station. Drought frequency (DF) is expressed as Equation (2) (Spinoni et al., 2014; Wang et al., 2018b):

$$DF = \frac{n_m}{N_m} \times 100\% \quad (2)$$

where n_m is the number of the drought months, and N_m is the total number of months. Drought intensity (DI) was calculated via Equation (3) (Wang et al., 2018a; Haile et al., 2020b):

$$DI = \left| \frac{1}{n} \sum_{i=1}^{n} DInd_i \right| \quad (3)$$

where, n is the number of drought events, and $DInd_i$ is the accumulated drought index values below the threshold (-1) for drought events i^{th}.

2.3.2. Drought propagation

Here, three characteristics of drought propagation including propagation time (i.e. response time scale), propagation rate, and lag time, were analyzed. The propagation time between MDIs (i.e. SPI and SPEI) with various timescales, ADIs (SSI1 and SSI2), and their correlations were analyzed using the Pearson correlation coefficient (r). Here, r between the time series of SSI1 (i.e. SSI2) and SPI_n (i.e. $SPEI_n$) was first calculated, where n is a time scale of 1–48 months. Next, the time scale *m* corresponding to the peak correlation coefficient between SPI_m (i.e. $SPEI_m$) and SSI1 (SSI2) was identified as the propagation time or response time scale, with the response time scale *m* indicating the accumulated precipitation deficiency in the previous *m* months leading to soil moisture deficits (Zhang et al., 2022b).

Various types of droughts have different periods including onset, persistence, peak, recovery, and termination stages. These periods can be used to determine the lag time between MD and other

198 drought types (e.g., agricultural, hydrological, etc.). The lag time between the beginning of two
199 different drought types (meteorological and agricultural drought) shows the onset of drought
200 propagation (Sattar et al., 2019; Bhardwaj et al., 2020).

201 The changes in drought properties (e.g., frequency, intensity, duration, and number of events)
202 or property percentages of drought types can be defined as the propagation rate. The propagation
203 rate from MD to AD can be expressed as follows (Sattar et al., 2019; Bhardwaj et al., 2020; Zhou
204 et al., 2021; Zhang et al., 2022b):

$$R_p = a_p / m_p \quad (4)$$

205 Where R_p is the propagation rate for special drought properties (e.g. NDE, DD, DF, and DI); a_p
206 is the number of AD events; m_p is the total number of MD events during the entire period. In the
207 study, propagation rates were calculated through four drought properties (e.g. NDE, DD, DF, and
208 DI) between pairwise estimates of MDI_s (SPI and SPEI) and ADI_s (SSI1 and SSI2) in all grids.

209

210 *2.3.3. Drought events based on Global Drought Observatory and in-situ data*

211 This section aims to find the substantial meteoroidal drought events and associated AD events.
212 The Global Drought Observatory (GDO; http://edo.jrc.ec.europa.eu/gdo/) uses both the SPI and
213 the SPEI at 3-, 6-, and 12-month time scales between 1951 and 2016 in country scale (Spinoni et
214 al., 2019). A drought event in the GDO procedure starts when for at least two consecutive months,
215 the analyzed indices (e.g., SPI or SPEI) fall below the figure related to a certain negative standard
216 deviation (e.g., SPEI3 < $-\sigma$) and comes to an end with the index goes over 0. To validate GDO's
217 reported drought events, the anomalies of P and PET based on measured datasets in synoptic
218 stations were analyzed during 1987–2019 (Fig. 3).

219

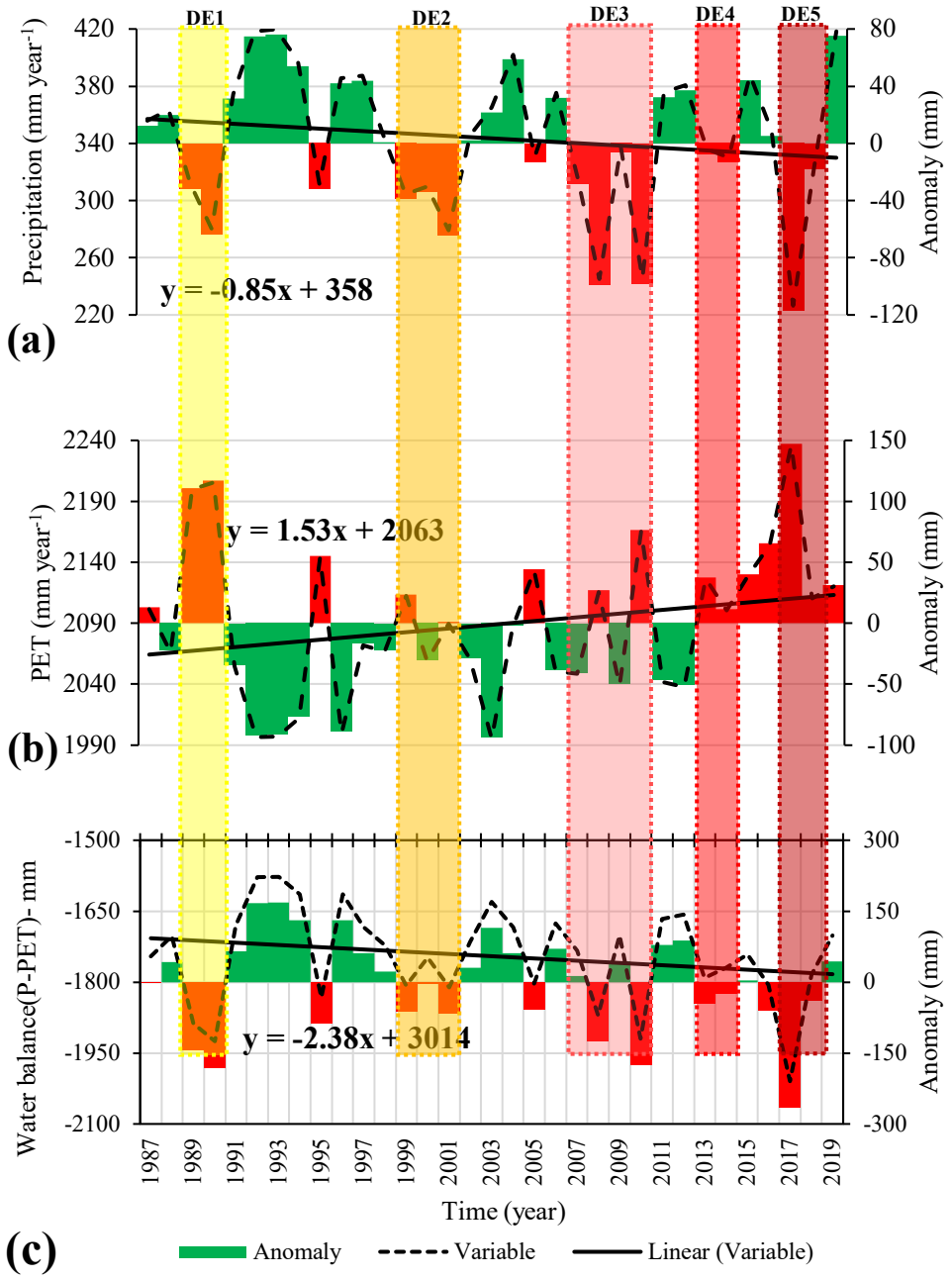

Fig. 3. Yearly and anomaly variation of P (a), PET (b) and water balance (P-PET) during 1987–2019 in Iran

Fig. 3 indicates the downward trend of P and the upward trend of PET resulting in the water trend (deference between P and PET). Here, two or more consecutive years with precipitation values less than the long-term average were considered drought events. Accordingly, five drought

events were identified during 1989–1990 / 1999–2001 / 2007–2010 / 2013–2014 and 2017–2019, respectively. Moreover, according to GDO reports, 12 events based on SPEI12 and 10 events based on SPI12 occurred during 1951–2016 across Iran. The widest and longest events occurred during 1999–2000 / 2008–2009 / 2014–2015, respectively. These drought events were also authenticated by the results of other studies (Behrang Manesh et al., 2019; Nouri and Homaee, 2020; Rezaei, 2021). Here, MD events were determined based on indicators that are commonly employed for identifying drought (He et al., 2016).

3. Results and Discussion

3.1. Propagation time

Correlation analysis between drought indices is a popular method to understand drought propagation. Fig. 4 shows the cross-correlations using the Pearson correlation coefficient between SPI, SPEI, SSI1, and SSI2 over 1-, 3-, 6-, 9-, 12-, 18-, 24-, and 48-month periods. A notable variation can be seen in the correlation values between the indices across different basins, with the highest correlation observed in the MKN basin (code 26) at 0.85 and the lowest in the GKH basin (code 42) at 0.44. Averaging the correlations across the HA, AR, SA, and HU basins yielded values of 0.70, 0.68, 0.69, and 0.61, respectively, indicating a downward trend in the correlation between MD and AD indices from HA to HU climates.

Additionally, the Pearson correlation coefficient exhibited an upward trend from the 1-month to the 48-month time scales for most indices. The mean *r* in the basins for 1-, 3-, 6-, 9-, 12-, 18-, 24-, and 48-month periods was calculated at 0.41, 0.48, 0.59, 0.71, 0.81, 0.74, 0.82, and 0.88, respectively. The observed upward trend in the Pearson correlation coefficient from the 1-month to the 48-month time scales for most indices indicates that as the temporal resolution increases, the relationship between the different drought indices

strengthens. This may be attributed to the smoothing effect of averaging over a longer period, which reduces variability and allows for more consistent patterns to emerge.

Analysis of the average PCC values illustrated an ascending trend from SPI-SSI2, SPI-SSI1, SPEI-SSI2, SPEI-SSI1, SSI1-SSI2 to SPI-SPEI, ranging from 0.51, 0.59, 0.61, 0.69, 0.83 to 0.84, across all basins, respectively. The low correlation of SPI-SSI1 and SPI-SSI2 on short time scales may be due to the differing time sensitivities of these indices. The SPI focuses on precipitation anomalies over varying periods, while SSI measures soil moisture conditions. On shorter time scales, these measurements may reflect different hydrological processes, leading to weak correlations.

The better correlation between SSI1 and SSI2 in semiarid basins compared to hyperarid basins can be attributed to the more pronounced seasonal fluctuations in soil moisture and evapotranspiration in semiarid regions. In hyperarid environments, consistent moisture deficits typically limit variability in soil moisture indices, resulting in lower correlation.

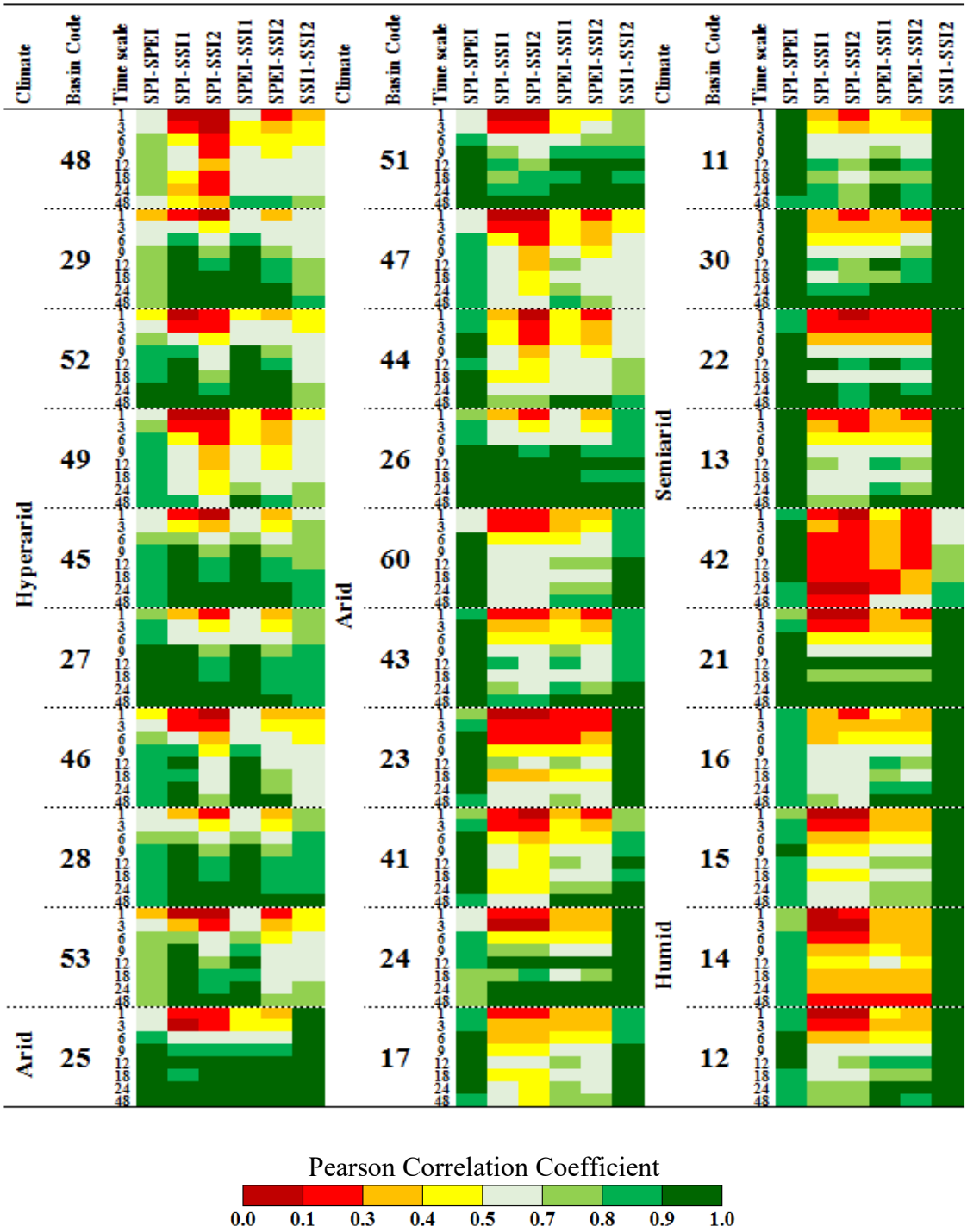

Fig. 4. Heat map of Pearson correlation coefficient between multi-time scales of drought indices in 30 basins.

264

265 To calculate the propagation time from MD to AD, the PCC of SPI at different scales (1 to 48

266 months) and SSI11 and SSI21 were computed for each basin, selecting the maximum coefficient

value as the propagation time in each basin. The mean propagation time from MD to AD was subsequently calculated for each basin based on these values (Dai et al., 2022b; Zhang et al., 2022a). Fig. 5 presents the propagation time of basins and the Pearson correlation coefficient of pixels between MDIs (SPI and SPEI) and ADIs (SSI1 and SSI2).

This examination of the correlation and propagation times highlights the complicated relationship between agricultural and meteorological drought indices, elucidating the varying degrees of interdependence between these indices across different climate zones. Understanding these nuances is crucial for formulating targeted strategies for drought management and preparedness. The observed trends emphasize the need for adaptable and region-specific policies to effectively mitigate the adverse impacts of drought on agriculture and water resource sustainability, especially in regions prone to prolonged drought events.

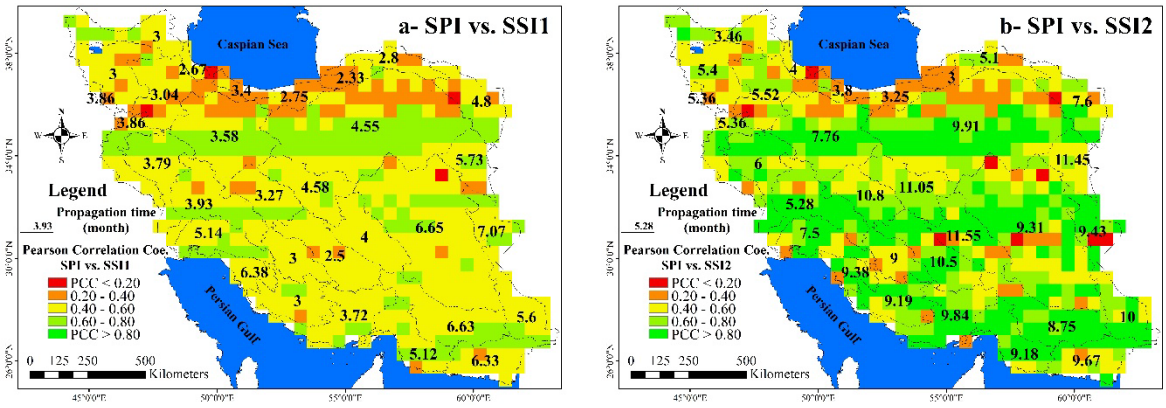

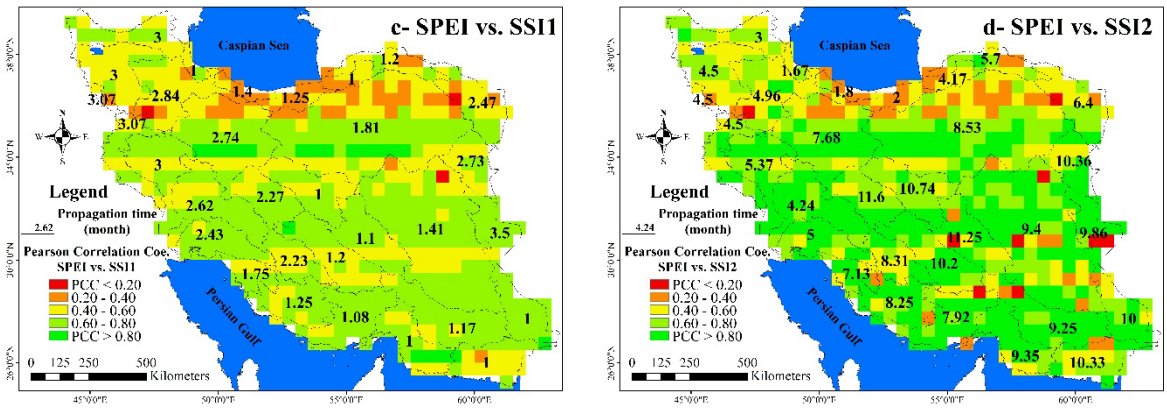

Fig. 5. Propagation time and Pearson correlation coefficient of (a) SPI-SSI1, (b) SPI-SSI2, (c) SPEI-SSI1, and (d) SPEI-SSI2 in Iran's basins.

The average propagation time in HA, AR, SA, and HU basins was achieved at 6.63, 5.51, 4.22, and 2.42 months, respectively, illustrating an increasing response time in the propagation of AD to MD from humid (HU) to hyper-arid (HA) climates. Moreover, the correlation coefficient values between the ADIs (SSI1 and SSI2) and the meteorological index (SPI) exhibit an upward trend from HU (0.44) climate to HA (0.75) climate.

According to Fig. 5, the average propagation times in SPEI-SSI1 (1.88 months) and SPI-SSI1 (4.21 months) are the shortest, while those of SPEI-SSI2 (7.12 months) and SPI-SSI2 (7.73 months) are the longest. Additionally, the PCC increases from SPI-SSI1 (0.51) and SPEI-SSI1 (0.59) to SPI-SSI2 (0.65) and SPEI-SSI2 (0.70) in all of the studied basins. These observations suggest that the propagation time and correlation coefficient between MDIs (SPI and SPEI) and ADIs (SSI1 and SSI2) show an increasing trend from the first layer (SSI1) to the second layer (SSI2) of soils.

The differences in average propagation times between SPEI-SSI1 (1.88 months) and SPI-SSI1 (4.21 months) can be explained by the influences of potential evapotranspiration. SPEI incorporates both precipitation and potential evapotranspiration, making it more sensitive to

294 changes in water balance over time. In contrast, SPI focuses solely on precipitation, which may
295 lead to longer lag times in reflecting soil moisture conditions.

296 The observed trends in propagation times and correlation coefficients highlight the intricate
297 interplay between various drought indices and soil layers, emphasizing the complexity of the
298 relationship between meteorological conditions and subsequent soil moisture dynamics. These
299 findings underscore the importance of considering soil characteristics and layers in assessing
300 drought propagation, especially in regions with varying soil properties. Such insights are crucial
301 for the development of targeted and effective strategies for agricultural planning and water
302 resource management, particularly in regions vulnerable to prolonged drought events and soil
303 moisture fluctuations.

304 *3.2. Lag time*

305 According to meteorological (SPI and SPEI) and agricultural (SSI1 and SSI2) drought indices
306 at multiple timescales (i.e., 1, 3, 6, 9, 12, 18, 24, and 48-month periods), values below a threshold
307 of -1 were selected as drought events. The analysis showed the presence of three distinct classes
308 of drought, including moderate, severe, and extreme, across all grids and the research period (Fig.
309 6). Drought events were determined to occur if the drought index fell below the designated
310 threshold (-1) for a minimum of three successive months.

311 Based on SPI and SPEI analyses, three significant drought events, namely DE1, DE2, and DE3,
312 were identified during the periods Mar 2000 to Mar 2002, Mar 2008 to Mar 2009, and Dec 2017
313 to Dec 2018, respectively, in different timescales. However, as shown in Figs. 6c and d, the
314 analysis of SSI1 and SSI2 demonstrated a relatively lower number of AD events in all grids over
315 the research period.

The findings from the analysis of drought events using various meteorological and agricultural indices underscore the intermittent yet impactful nature of drought occurrences, revealing distinct patterns of moderate, severe, and extreme droughts in the region over different timescales. The detection of specific drought occurrences through these indices yields valuable insights into the temporal dynamics of drought events and their potential implications for agricultural and environmental management. Furthermore, the comparative analysis of meteorological and agricultural drought indices highlights their varying sensitivities to different drought events, emphasizing the importance of considering multiple indices for a comprehensive understanding of drought patterns and their impacts on the region's agricultural systems.

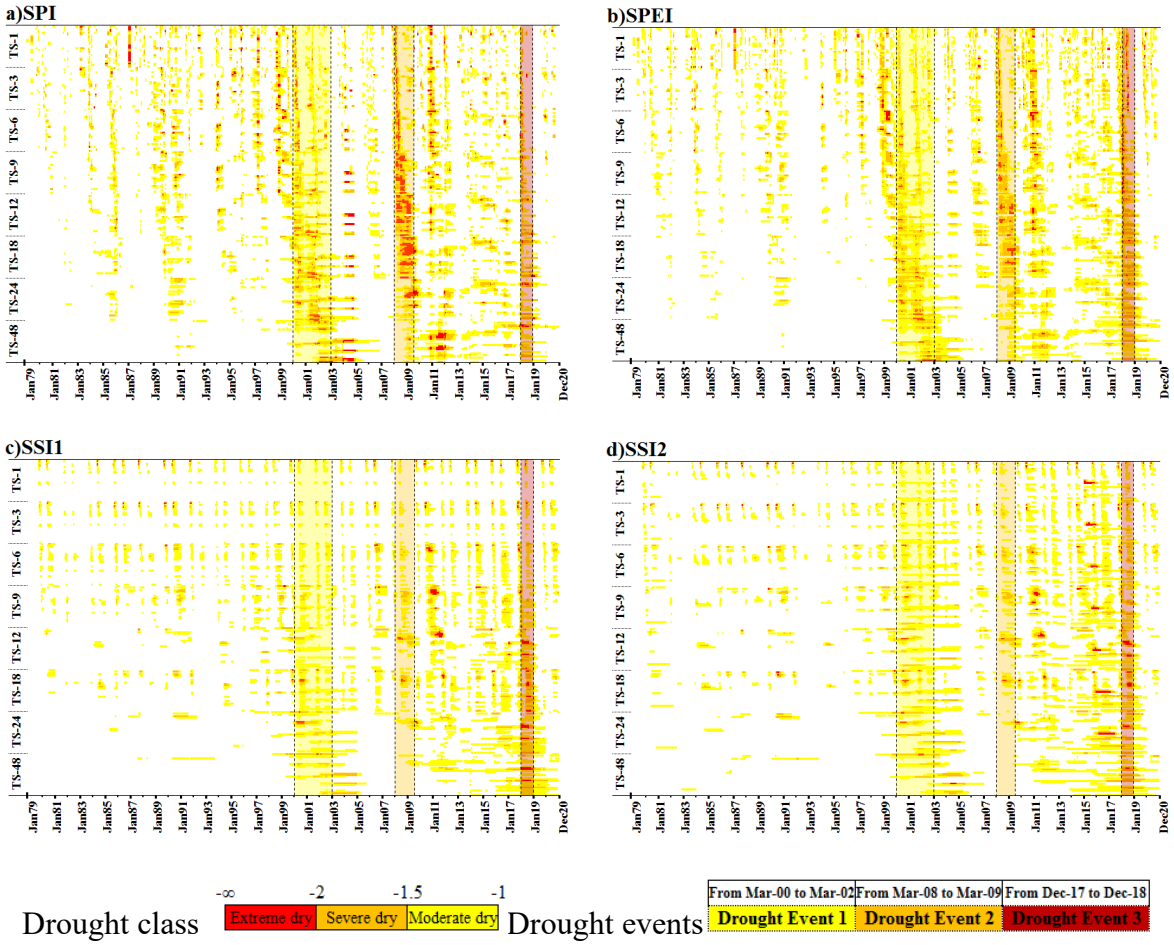

Fig. 6. Heat map of drought indices in multi-time scales during Jan79–Dec20 in 621 grids.

325

326 *3.2.1. Meteorological drought identification*

327 The first step in determining the lag time between MD and AD involves the identification of
328 specific drought occurrences based on the intensity of meteorological drought indices (MDIs) and
329 agricultural drought indices (ADIs). These drought events were classified into moderate, severe,
330 and extreme classes, as shown in Fig. 6. Additionally, the characteristics of the top MD events
331 were discerned across different climate zones in Iran and are detailed in Table 3.

332 Through a comprehensive analysis of Table 3 and Figure 6, three prominent MD events during
333 the 1979–2020 period in various climates of Iran were identified based on SPI and SPEI. The most
334 extended MD event, lasting 38 months, occurred from February 1999 to March 2002, affecting the
335 SA and HU regions of Iran (referred to as drought event 1). Previous research has highlighted the
336 significance of the 1999–2002 drought episode, emphasizing its regional impact across various
337 parts of Asia (Malik et al., 2013; Adnan et al., 2018). Furthermore, the second significant drought
338 event (drought event 2), covering the largest area percentage (97%), transpired from April 2008 to
339 March 2009 in the HU regions of Iran. More recently, another notable MD event (drought event
340 3) occurred during the years 2017–2019 across Iran.

341 The insights derived from the analysis of these top MD events shed light on the temporal
342 characteristics and geographical extent of severe drought occurrences in various climate zones of
343 Iran. Understanding the dynamics and impacts of these prolonged drought events is vital for
344 implementing effective mitigation strategies and policy interventions to minimize the adverse
345 effects on agricultural productivity and water resource management. Furthermore, the
346 identification of specific timeframes and geographical areas affected by these drought events

provides crucial information for developing region-specific resilience measures and adaptive strategies to address the challenges posed by recurring and prolonged drought conditions.

Table 3. Top meteorological drought events in different climates of Iran.

Drought event	Drought index	Climate class	Onset	Termination	Duration (month)	Severity	Intensity	Peak	Area (%)
Drought event 1 (The longest event)	SPI-12	HA	Mar-00	Dec-02	34	-37.1	-1.09	-2.21	59
		AR	Mar-00	Feb-02	24	-23.5	-0.98	-2.21	51
		SA	Feb-99	Mar-02	38	-41.1	-1.08	-2.21	62
		HU	Feb-99	Jan-02	36	-30.2	-0.84	-1.70	31
	SPEI-12	HA	Mar-00	Dec-02	34	-39.5	-1.16	-2.32	67
		AR	Mar-00	Mar-02	25	-28.5	-1.14	-2.18	63
		SA	Feb-99	Mar-02	38	-48.4	-1.27	-2.30	73
		HU	Feb-99	Mar-02	38	-40.2	-1.06	-1.80	53
Drought event 2 (The widest event)	SPI-12	HA	Mar-08	Feb-09	12	-16.0	-1.33	-2.21	82
		AR	Mar-08	Mar-09	13	-24.1	-1.85	-2.22	95
		SA	Apr-08	Mar-09	12	-21.9	-1.82	-2.20	94
		HU	Apr-08	Mar-09	12	-22.0	-1.84	-2.20	97
	SPEI-12	HA	Mar-08	Feb-09	12	-14.3	-1.19	-2.04	65
		AR	Mar-08	Mar-09	13	-22.3	-1.72	-2.32	98
		SA	Apr-08	Mar-09	12	-20.2	-1.68	-2.41	90
		HU	Apr-08	Mar-09	12	-19.2	-1.60	-2.00	97
Drought event 3	SPI-12	HA	Jan-18	Dec-18	12	-14.1	-1.17	-2.16	58
		AR	Mar-18	Sep-18	7	-7.3	-1.05	-2.13	56
		SA	Dec-17	Mar-18	3	-2.4	-0.82	-2.00	38
		HU	Dec-17	Nov-18	12	-18.1	-1.51	-2.20	75
	SPEI-12	HA	Apr-17	Feb-19	23	-31.7	-1.38	-2.20	82
		AR	Jan-18	Oct-18	10	-13.4	-1.34	-2.38	85
		SA	Dec-17	Apr-18	5	-6.3	-1.26	-2.00	69
		HU	Sep-17	Jan-19	17	-25.7	-1.51	-2.20	84

3.2.2. Agricultural drought identification

Agricultural drought events, which corresponded to the meteorological drought (MD) occurrences in 1999–2002, 2008–2009, and 2017–2019 (refer to Table 3), were evaluated based on the threshold of -1 for the SSI1 and SSI2 indices, as outlined in Table 4. The characteristics of these agricultural drought events were identified, providing critical insights into the effects of prolonged meteorological droughts on agricultural systems and soil moisture dynamics.

The onset of agricultural drought (AD) exhibited varying lag times ranging from 2 to 6 months across different climate classes in Iran. Notably, the lag times from MD to AD showed an increasing trend from humid (HU) to hyper-arid (HA) climates. In HU climates, the propagation of drought occurred much more rapidly compared to arid (AR) climates, with a lag time of less than 3 months from MD to AD. Conversely, in HA and AR climates, the lag time ranged from 2–6 months, which was 1–3 months longer than that observed in HU climates.

These results are aligned with the conclusions drawn from previous studies (Huang et al., 2021b; Xu et al., 2021, 2023), highlighting the quicker propagation of drought events (i.e., shorter response time scales) in HU climates and slower propagation (i.e., longer response time scales) in AR climates. Tables 3 and 4 also illustrate that during the propagation process from MD to AD, the severity (intensity or peak) of the drought events reduced, while the duration increased. Zhu et al. (2021) similarly analyzed the propagation from MD to AD through SPEI and soil moisture, indicating that the duration of AD generally surpassed that of MD in most regions across the world.

These findings underscore the intricate relationship between meteorological and agricultural drought events and emphasize the critical role of climatic variations in influencing the propagation dynamics of drought events. Understanding the nuanced interplay between meteorological and agricultural droughts is crucial for developing targeted schemes dedicated to agricultural resilience and water resource management, particularly in regions vulnerable to the adverse impacts of prolonged drought conditions.

Table 4. Top agricultural drought events in different climates of Iran.

Drought Event	Drought Index	Climate class	Onset	Termination	Duration (month)	Severity	Intensity	Peak	Area(%)
Drought event 1	SSI1-12	HA	Apr-00	Mar-03	35	-27.85	-0.87	-1.36	45
		AR	May-00	Jun-02	25	-11.51	-0.64	-1.60	28
		SA	Apr-99	May-02	38	-35.58	-1.08	-2.00	53
		HU	May-99	Apr-02	36	-5.70	-0.57	-1.10	27
	SSI2-12	HA	May-00	Apr-03	36	-24.60	-0.98	-1.52	60
		AR	Jun-00	Jul-02	25	-11.20	-0.70	-1.75	30
		SA	May-99	Jun-02	38	-37.10	-1.06	-1.80	56
		HU	May-99	May-02	37	-2.17	-0.72	-1.20	44
Drought event 2	SSI1-12	HA	Apr-08	Jun-09	14	-2.59	-0.46	-1.29	41
		AR	Apr-08	Jun-09	14	-11.95	-0.92	-1.86	58
		SA	Jun-08	May-09	11	-14.68	-1.22	-1.90	70
		HU	Jun-08	May-09	11	-8.20	-0.68	-1.80	48
	SSI2-12	HA	Apr-08	Apr-09	12	-2.43	0.12	-1.32	42
		AR	Apr-08	May-09	13	-7.25	-0.91	-1.80	48
		SA	May-08	May-09	12	-12.26	-1.11	-2.10	66
		HU	Jun-08	May-09	11	-6.43	-0.71	-1.80	43
Drought event 3	SSI1-12	HA	Feb-18	Jan-19	11	-13.23	-1.27	-1.58	45
		AR	Apr-18	Dec-18	8	-4.97	-1.60	-1.79	47
		SA	Jan-18	Apr-18	3	-2.24	-1.06	-1.70	30
		HU	Feb-18	Dec-18	10	-12.07	-1.51	-1.90	72
	SSI2-12	HA	May-17	May-19	24	-9.36	-0.72	-1.54	59
		AR	Feb-18	Jan-19	11	-10.93	-1.30	-1.69	67
		SA	Jan-18	Jun-18	5	-5.39	-0.84	-1.66	53
		HU	Nov-17	Feb-19	15	-16.13	-1.47	-2.00	77

3.3. Propagation rate

In addition to examining the MD and AD propagation times (DPT), this study explored the relationships between these drought types through the analysis of various properties, such as the number of events (NDE), frequency (DF), duration (DD), and intensity (DI) (Zhang et al., 2022b). The drought propagation rate (DPR), defined as the percentage change in properties between different drought types (Sattar et al., 2019), was employed to assess the sensitivity and response of agricultural drought (AD) to meteorological drought (MD) events.

For the two series of drought indices (MDIs and ADIs) analyzed in this study, the drought characteristics (NDE, DD, DF, and DI) were extracted based on a specific threshold (set at -1). The propagation rate for the SSI1 & SSI2 and SPI & SPEI at 3-, 6-, 9-, and 12-month time scales were calculated for each grid within the basins. Fig. 7 displays the box plot of the DPR for the various drought characteristics across all studied basins.

DPR values generally ranged from 0 to 1, with higher values indicating a heightened sensitivity or strong response of AD to MD events (Zhang et al., 2022b). The analysis of the propagation rate based on the number of drought events revealed the influence of meteorological droughts in triggering subsequent agricultural droughts (Guo et al., 2019).

Fig. 7a illustrates the observed increase in the propagation rate of NDE from hyper-arid (HA) to humid (HU) basins. Notably, the propagation rate exceeding 1 signifies that the properties of agricultural droughts (i.e., NDE, DF, DD, and DI) surpassed those of meteorological droughts. Therefore, the findings presented in Figure 7a highlight the increasing sensitivity of agricultural droughts to meteorological droughts from arid (AR) to humid (HU) basins. This suggests that meteorological droughts in humid regions trigger more significant agricultural drought events compared to arid regions. The corresponding DPR values are presented in Table 5, detailing the propagation rates for various climates and their implications for drought sensitivity and response dynamics.

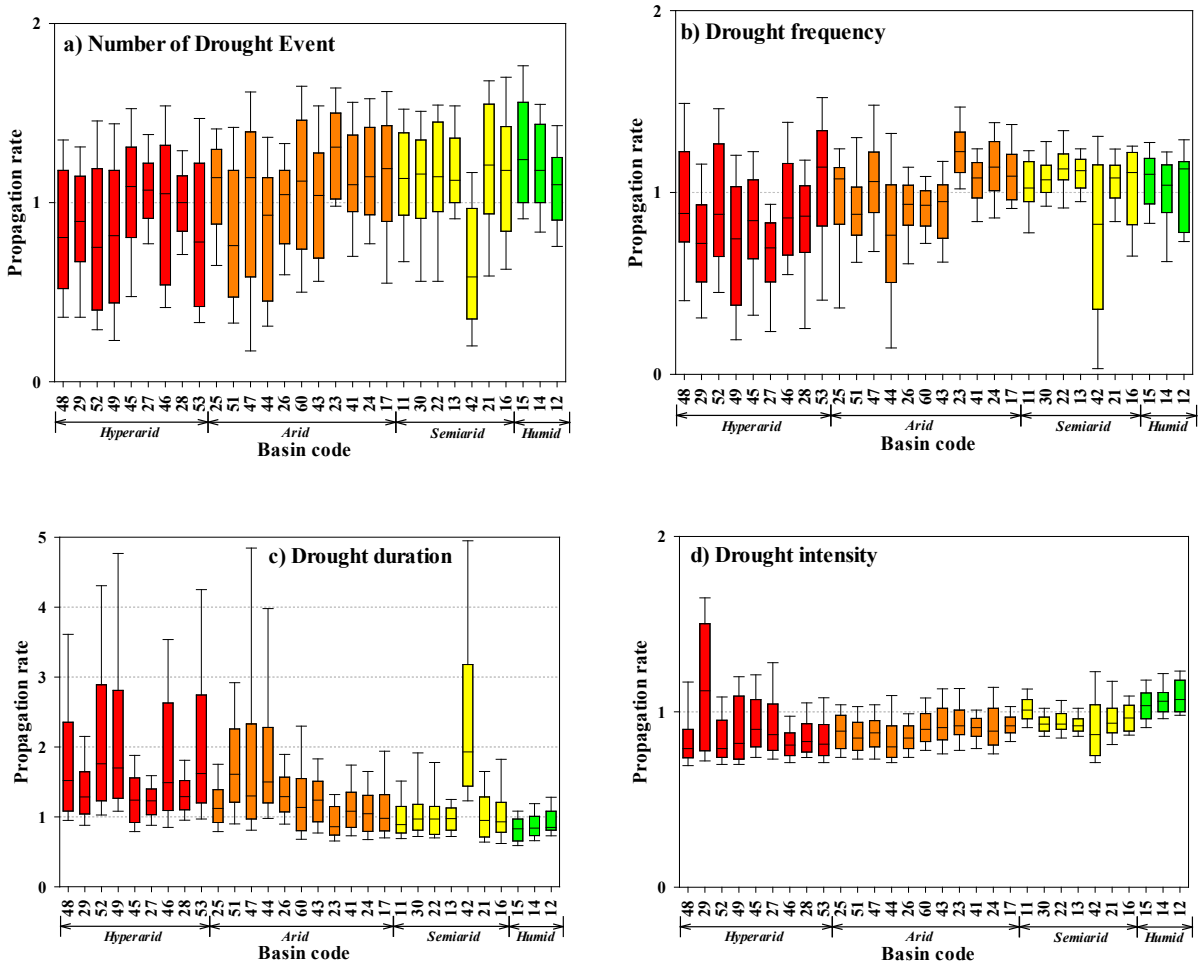

Fig. 7. Box plots of the drought propagation rate for a) number of events, b) frequency, c) duration, and d) intensity in all basins categorized into climates.

406

407 The propagation rate values presented in Table 5 have been organized into three distinct
408 categories to facilitate comprehension: values less than or equal to 1 (highlighted in green), values
409 between 1 and 2 (highlighted in yellow), and values greater than 2 (highlighted in red). These
410 color-coded distinctions aid in understanding the varying degrees of sensitivity or response of AD
411 to MD across different climates. Notably, higher propagation rate values indicate a heightened Ad
412 to MD sensitivity in these diverse climatic zones. Additionally, a propagation rate greater than 1

signifies an increase in certain drought characteristics, such as the number of events (NDE), frequency (DF), duration (DD), or intensity (DI), from MD to AD.

Overall, the propagation rate values for drought characteristics (NDE, DF, DD, and DI) demonstrate remarkable consistency across different timescales, with values remaining relatively similar except at the 12-month timescale in some cases. The findings suggest a general trend of increasing propagation rates from shorter (3-month) to longer (12-month) timescales, signifying the amplification of the sensitivity or response of AD to MD over extended periods.

In Table 5, the analysis reveals that the maximum and minimum propagation rate values correspond to the duration (DD) and intensity of drought events (DI), respectively. This observation indicates that while the duration of drought events from MD to AD has increased significantly (with propagation rate values greater than 1), the intensity of these drought events has shown a notable decrease (with propagation rate values less than 1) across the majority of grids. Furthermore, the propagation rates exhibit an increasing trend from hyper-arid (HA) to humid (HU) climates for all drought characteristics, with the exception of drought duration. This suggests that the AD to MD sensitivity or response is particularly high in humid climates compared to hyper-arid climates.

Table 5. Propagation rate at multi-time scales for different climates of case study.

DC	Climate	Hyper arid				Arid				Semiarid				Humid			
	TS	3	6	9	12	3	6	9	12	3	6	9	12	3	6	9	12
NDE	SSI1/SPI	1.1	1.2	1.1	0.8	1.1	1.4	1.3	0.7	1.1	1.5	1.4	0.7	1.0	1.4	1.5	0.9
	SSI2/SPI	0.6	0.6	0.6	0.6	0.9	1.0	0.9	0.5	1.0	1.2	1.1	0.6	1.0	1.3	1.4	0.9
	SSI1/SPEI	1.2	1.5	1.4	1.0	1.1	1.5	1.4	0.8	1.1	1.4	1.4	0.7	1.0	1.3	1.6	1.0
	SSI2/SPEI	0.6	0.7	0.7	0.7	0.9	1.1	0.9	0.6	1.0	1.2	1.1	0.6	1.0	1.3	1.5	0.9
DF	SSI1/SPI	0.2	0.3	0.7	0.9	0.5	1.0	1.0	1.0	1.1	1.1	1.0	1.0	1.2	1.2	1.1	1.1
	SSI2/SPI	0.9	0.8	0.9	1.0	0.9	1.0	1.0	1.1	1.2	1.1	1.1	1.1	1.2	1.2	1.1	1.1
	SSI1/SPEI	0.2	0.3	0.6	0.8	0.5	0.9	0.9	0.9	1.0	1.0	0.9	0.9	1.1	1.1	1.0	0.9
	SSI2/SPEI	0.7	0.8	0.8	0.8	0.8	0.9	0.9	0.9	1.1	1.0	1.0	0.9	1.1	1.1	1.0	0.9

DD	SSI1/SPI	1.6	1.1	1.1	1.5	1.3	0.9	0.9	1.6	1.1	0.8	0.8	1.7	1.0	0.8	0.7	1.1
	SSI2/SPI	3.1	2.5	2.3	2.0	1.8	1.4	1.6	2.2	1.6	1.2	1.3	2.1	1.0	0.8	0.7	1.2
	SSI1/SPEI	1.3	0.9	0.9	1.3	1.2	0.9	0.9	1.5	1.1	0.8	0.8	1.7	0.9	0.8	0.7	1.0
	SSI2/SPEI	2.4	1.9	1.8	1.8	1.6	1.3	1.5	2.1	1.5	1.2	1.3	2.0	0.9	0.8	0.7	1.1
DI	SSI1/SPI	0.1	0.6	0.8	0.8	0.6	0.8	0.9	0.9	0.8	0.9	0.9	1.0	1.1	1.0	1.0	1.1
	SSI2/SPI	0.9	0.9	0.9	0.9	0.9	0.9	0.9	0.9	0.9	0.9	1.0	1.0	1.1	1.0	1.0	1.0
	SSI1/SPEI	0.1	0.6	0.8	0.8	0.6	0.8	0.9	0.9	0.8	0.9	0.9	1.0	1.1	1.0	1.1	1.1
	SSI2/SPEI	0.9	0.9	1.0	1.0	0.9	0.9	1.0	1.0	0.9	0.9	1.0	1.0	1.1	1.0	1.1	1.1

Various climate regions exhibited distinct primary drivers for agricultural and meteorological droughts due to their unique climate characteristics (Ding et al., 2021; Sun et al., 2023). In humid climatic regions, the hydrological cycle is initiated by water transport. Regions like southern Iran, characterized by humid climates, are more susceptible to the effect of meteorological drought on agricultural or surface water drought. This finding aligns with results reported in earlier studies (e.g., Liu et al., 2023). In a study by Han et al. (2023), the key factors influencing the dynamics of drought trigger thresholds were recognized as the aridity index and temperature. The study's findings illustrated the diverse impacts of the aridity index on drought propagation across various climates.

4. Conclusion

The analysis of lag time from MD to AD necessitates the identification of primary drought events during the research period within each climate type. Firstly, the top MD events were identified based on SPI-12 and SPEI-12 from 1979 to 2021 using GDO reports. Three notable MD events were then pinpointed, occurring in 1999–2002, 2008–2009, and 2017–2019 in various regions of Iran. Subsequently, the characteristics of these events, including onset, duration, termination, severity, peak, and area, were differentiated across different climatic zones. In addition, the attributes of the AD events were determined based on SSI1 and SSI2 at various time scales in each grid. Consequently, the difference in months from the onset of MD to the

corresponding AD was designated as the lag time. The findings revealed that the lag time from MD to AD ranged from 2 to 6 months in different climates in Iran. This conclusion reinforces the results obtained for propagation time and emphasizes that the gap between the onset of MD and AD in humid climates is 1 to 3 months shorter compared to arid climates. These findings are in line with those of earlier studies (Xu et al., 2021, 2023).

Furthermore, the propagation rates for MD and AD drought characteristics, namely the number of drought events (NDE), frequency (DF), duration (DD), and intensity (DI), were computed based on these drought indices (i.e., SPI, SPEI, SSI1, and SSI2) at multiple time scales for all grids in the case study. The analysis indicated that during the propagation of MD, the number of events and frequency of AD decreased, while the duration increased in most basins, though there were exceptions, as discovered by previous studies (Li et al., 2020; Zhu et al., 2021). Overall, the propagation rates exceeding 1 in humid climates suggest that AD in such regions exhibits a heightened sensitivity to MD compared to arid climates.

Drought propagation analysis presents various challenges owing to the complexity of the processes involved. Some of these challenges are uncertainty in global gridded databases, methodological discrepancy, and the influence of diverse factors. To address these challenges, several recommendations are proposed. Firstly, the calculation of agricultural drought indices based on soil moisture necessitates reliable and comprehensive datasets of soil moisture measurements, which are often scarce, particularly in regions like the case study in Iran. Utilizing measured soil moisture data sourced from the International Soil Moisture Network (Dorigo et al., 2021) can enhance the accuracy of drought propagation results. Moreover, employing alternative methods, especially nonlinear response methods, is advised to investigate the propagation time from MD to AD, given the potential disparities in results from different approaches. Finally, as

drought propagation is influenced by various factors with distinct roles, it is crucial for future studies to focus on discerning the role of these factors, especially those related to human-induced conditions, to attain a more comprehensive understanding of drought propagation dynamics.

It is important to recognize that the relationship between drought propagation and basins with diverse climate conditions may be influenced by additional factors, including teleconnection factors, land cover, and land use (Han et al., 2019; Zhang et al., 2021b). Consequently, a more thorough examination of the factors impacting the propagation relationships in every basin with varying climatic conditions is warranted in future research.

Invest in research to develop drought-resistant crop varieties and sustainable agricultural practices. This includes funding for agricultural extension services to educate farmers on best practices for drought management. Establish comprehensive monitoring systems that integrate meteorological data with agricultural indicators. This can help in early detection of drought conditions and facilitate timely interventions.

References

Ababaei B (2020) Spatio-Temporal Variations of Seven Weather Variables in Iran: Application of Cru Ts and Gpcc Data Sets†. Irrig Drain 69:164–185. https://doi.org/10.1002/ird.2399

Afshar MH, Bulut B, Duzenli E, et al (2022) Global spatiotemporal consistency between meteorological and soil moisture drought indices. Agric For Meteorol 316:108848

Allen RG, Pruitt WO, Wright JL, et al (2006) A recommendation on standardized surface resistance for hourly calculation of reference ETo by the FAO56 Penman-Monteith method. Agric water Manag 81:1–22

Anvari S, Moghaddasi M (2023) Historical changes of extreme temperature in relation to soil moisture over different climatic zones of Iran. Stoch Environ Res Risk Assess 1–17

Araghi A, Jaghargh MR, Maghrebi M, et al (2021) Investigation of satellite-related precipitation products for modeling of rainfed wheat production systems. Agric Water Manag 258:. https://doi.org/10.1016/j.agwat.2021.107222

Araghi A, Martinez CJ, Adamowski J, Olesen JE (2018) Spatiotemporal variations of aridity in Iran using high-resolution gridded data. Int J Climatol 38:2701–2717. https://doi.org/10.1002/joc.5454

Araghi A, Martinez CJ, Olesen JE, Hoogenboom G (2022) Assessment of nine gridded temperature data for modeling of wheat production systems. Comput Electron Agric 199:. https://doi.org/10.1016/j.compag.2022.107189

Bae H, Ji H, Lim Y-J, et al (2019) Characteristics of drought propagation in South Korea: Relationship

between meteorological, agricultural, and hydrological droughts. Nat Hazards 99:1–16

Bazrafshan J, Cheraghalizadeh M (2021) Verification of abrupt and gradual shifts in Iranian precipitation and temperature data with statistical methods and stations metadata. Environ Monit Assess 193:139

Behrang Manesh M, Khosravi H, Heydari Alamdarloo E, et al (2019) Linkage of agricultural drought with meteorological drought in different climates of Iran. Theor Appl Climatol 138:1025–1033

Bhardwaj K, Shah D, Aadhar S, Mishra V (2020) Propagation of meteorological to hydrological droughts in India. J Geophys Res Atmos 125:e2020JD033455

Cai S, Song X, Hu R, et al (2021) Spatiotemporal characteristics of agricultural droughts based on soil moisture data in Inner Mongolia from 1981 to 2019. J Hydrol 603:127104

Collins B, Ramezani Etedali H, Tavakol A, Kaviani A (2021) Spatiotemporal variations of evapotranspiration and reference crop water requirement over 1957–2016 in Iran based on CRU TS gridded dataset. J Arid Land 13:858–878. https://doi.org/10.1007/s40333-021-0103-4

Dai M, Huang S, Huang Q, et al (2022a) Propagation characteristics and mechanism from meteorological to agricultural drought in various seasons. J Hydrol 610:127897

Dai M, Huang S, Huang Q, et al (2022b) Propagation characteristics and mechanism from meteorological to agricultural drought in various seasons. J Hydrol 610:. https://doi.org/10.1016/j.jhydrol.2022.127897

Ding Y, Gong X, Xing Z, et al (2021) Attribution of meteorological, hydrological and agricultural drought propagation in different climatic regions of China. Agric Water Manag 255:106996. https://doi.org/10.1016/j.agwat.2021.106996

Dorigo W, Himmelbauer I, Aberer D, et al (2021) The International Soil Moisture Network: serving Earth system science for over a decade. Hydrol earth Syst Sci 25:5749–5804

Gibson AJ, Verdon-Kidd DC, Hancock GR, Willgoose G (2020) Catchment-scale drought: capturing the whole drought cycle using multiple indicators. Hydrol Earth Syst Sci 24:1985–2002

Guo H, Bao A, Liu T, et al (2019) Determining variable weights for an Optimal Scaled Drought Condition Index (OSDCI): Evaluation in Central Asia. Remote Sens Environ 231:111220. https://doi.org/10.1016/j.rse.2019.111220

Haile GG, Tang Q, Hosseini-Moghari S-M, et al (2020a) Projected impacts of climate change on drought patterns over East Africa. Earth's Futur 8:e2020EF001502

Haile GG, Tang Q, Hosseini-Moghari S-MM, et al (2020b) Projected Impacts of Climate Change on Drought Patterns Over East Africa. Earth's Futur 8:1–23. https://doi.org/10.1029/2020EF001502

Han Z, Huang S, Huang Q, et al (2021) GRACE-based high-resolution propagation threshold from meteorological to groundwater drought. Agric For Meteorol 307:108476

Han Z, Huang S, Huang Q, et al (2019) Propagation dynamics from meteorological to groundwater drought and their possible influence factors. J Hydrol 578:124102

Han Z, Huang S, Zhao J, et al (2023) Long-chain propagation pathways from meteorological to hydrological, agricultural and groundwater drought and their dynamics in China. J Hydrol 625:130131. https://doi.org/10.1016/j.jhydrol.2023.130131

Hao Z, AghaKouchak A (2014) A nonparametric multivariate multi-index drought monitoring framework. J Hydrometeorol 15:89–101

Harris I, Osborn TJ, Jones P, Lister D (2020) Version 4 of the CRU TS monthly high-resolution gridded multivariate climate dataset. Sci data 7:109

He J, Yang X, Li Z, et al (2016) Spatiotemporal variations of meteorological droughts in China during 1961--2014: An investigation based on multi-threshold identification. Int J Disaster Risk Sci 7:63–76

Hersbach H, Bell B, Berrisford P, et al (2020) The ERA5 global reanalysis. Q J R Meteorol Soc 146:1999–2049

Huang S, Li P, Huang Q, et al (2017) The propagation from meteorological to hydrological drought and its potential influence factors. J Hydrol 547:184–195

Huang S, Zhang X, Chen N, et al (2021a) Drought propagation modification after the construction of the Three Gorges Dam in the Yangtze River Basin. J Hydrol 603:127138

Huang S, Zhang X, Chen N, et al (2021b) Drought propagation modification after the construction of the Three Gorges Dam in the Yangtze River Basin. J Hydrol 603:127138. https://doi.org/10.1016/j.jhydrol.2021.127138

Karamouz M, Nazif S, Falahi M (2012) Hydrology and hydroclimatology: principles and applications. CRC Press

Li R, Chen N, Zhang X, et al (2020) Quantitative analysis of agricultural drought propagation process in the Yangtze River Basin by using cross wavelet analysis and spatial autocorrelation. Agric For Meteorol 280:107809

Liu Y, Shan F, Yue H, et al (2023) Global analysis of the correlation and propagation among meteorological, agricultural, surface water, and groundwater droughts. J Environ Manage 333:117460. https://doi.org/10.1016/j.jenvman.2023.117460

Liu Z, Wang Y, Shao M, et al (2016) Spatiotemporal analysis of multiscalar drought characteristics across the Loess Plateau of China. J Hydrol 534:281–299

Madani K (2014) Water management in Iran: what is causing the looming crisis? J Environ Stud Sci 4:315–328

McKee TB (1995) Drought monitoring with multiple time scales. In: Proceedings of 9th Conference on Applied Climatology, Boston, 1995

McKee TB, Doesken NJ, Kleist J, others (1993) The relationship of drought frequency and duration to time scales. In: Proceedings of the 8th Conference on Applied Climatology. pp 179–183

Moshir Panahi D, Sadeghi Tabas S, Kalantari Z, et al (2021) Spatio-temporal assessment of global gridded evapotranspiration datasets across Iran. Remote Sens 13:1816

Nouri M, Homaee M (2020) Drought trend, frequency and extremity across a wide range of climates over Iran. Meteorol Appl 27:e1899

Rezaei A (2021) Ocean-atmosphere circulation controls on integrated meteorological and agricultural drought over Iran. J Hydrol 603:126928

Saemian P, Hosseini-Moghari S-M, Fatehi I, et al (2021) Comprehensive evaluation of precipitation datasets over Iran. J Hydrol 603:127054

Sattar MN, Jehanzaib M, Kim JE, et al (2020) Application of the hidden Markov bayesian classifier and propagation concept for probabilistic assessment of meteorological and hydrological droughts in

585 South Korea. Atmosphere (Basel) 11:1000

586 Sattar MN, Lee J-Y, Shin J-Y, Kim T-W (2019) Probabilistic characteristics of drought propagation from
587 meteorological to hydrological drought in South Korea. Water Resour Manag 33:2439–2452

588 Sharafi S, Ghaleni MM (2022) Spatial assessment of drought features over different climates and seasons
589 across Iran. Theor Appl Climatol 1–17

590 Sheffield J, Goteti G, Wen F, Wood EF (2004) A simulated soil moisture based drought analysis for the
591 United States. J Geophys Res Atmos 109:

592 Singh NK, Emanuel RE, McGlynn BL, Miniat CF (2021) Soil moisture responses to rainfall: Implications
593 for runoff generation. Water Resour Res 57:e2020WR028827

594 Spinoni J, Barbosa P, De Jager A, et al (2019) A new global database of meteorological drought events
595 from 1951 to 2016. J Hydrol Reg Stud 22:100593

596 Spinoni J, Naumann G, Carrao H, et al (2014) World drought frequency, duration, and severity for 1951--
597 2010. Int J Climatol 34:2792–2804. https://doi.org/10.1002/joc.3875

598 Sun H, Sun X, Chen J, et al (2023) Different types of meteorological drought and their impact on
599 agriculture in Central China. J Hydrol 627:130423. https://doi.org/10.1016/j.jhydrol.2023.130423

600 Tsiros IX, Nastos P, Proutsos ND, Tsaousidis A (2020) Variability of the aridity index and related
601 drought parameters in Greece using climatological data over the last century (1900--1997). Atmos
602 Res 240:104914

603 Um M-J, Kim Y, Jung K, et al (2022) Evaluation of drought propagations with multiple indices in the
604 Yangtze River basin. J Environ Manage 317:115494

605 Unesco (1979) Map of the world distribution of arid regions: Explanatory note. Unesco

606 Vicente-Serrano SM, Beguer\'\ia S, López-Moreno JI, et al (2010a) A multiscalar drought index sensitive
607 to global warming: the standardized precipitation evapotranspiration index. J Clim 23:1696–1718.
608 https://doi.org/10.1175/2009JCLI2909.1

609 Vicente-Serrano SM, Beguer\'\ia S, López-Moreno JI (2010b) A multiscalar drought index sensitive to
610 global warming: the standardized precipitation evapotranspiration index. J Clim 23:1696–1718

611 Vogt J V, Naumann G, Masante D, et al (2018) Drought risk assessment and management: A conceptual
612 framework

613 Wang D, Borthwick AG, He H, et al (2018a) A hybrid wavelet de-noising and Rank-Set Pair Analysis
614 approach for forecasting hydro-meteorological time series. Environ Res 160:269–281.
615 https://doi.org/10.1016/j.envres.2017.09.033

616 Wang F, Wang Z, Yang H, et al (2018b) Study of the temporal and spatial patterns of drought in the
617 Yellow River basin based on SPEI. Sci China Earth Sci 61:1098–1111.
618 https://doi.org/10.1007/s11430-017-9198-2

619 Weng Z, Niu J, Guan H, Kang S (2023) Three-dimensional linkage between meteorological drought and
620 vegetation drought across China. Sci Total Environ 859:160300

621 Xu Y, Zhang X, Hao Z, et al (2021) Characterization of agricultural drought propagation over China
622 based on bivariate probabilistic quantification. J Hydrol 598:.
623 https://doi.org/10.1016/j.jhydrol.2021.126194

Xu Y, Zhang X, Wang X, et al (2019) Propagation from meteorological drought to hydrological drought under the impact of human activities: A case study in northern China. J Hydrol 579:124147

Xu Z, Wu Z, Shao Q, et al (2023) From meteorological to agricultural drought: Propagation time and probabilistic linkages. J Hydrol Reg Stud 46:. https://doi.org/10.1016/j.ejrh.2023.101329

Zhang H, Ding J, Wang Y, et al (2021a) Investigation about the correlation and propagation among meteorological, agricultural and groundwater droughts over humid and arid/semi-arid basins in China. J Hydrol 603:127007

Zhang H, Ding J, Wang Y, et al (2021b) Investigation about the correlation and propagation among meteorological, agricultural and groundwater droughts over humid and arid/semi-arid basins in China. J Hydrol 603:. https://doi.org/10.1016/j.jhydrol.2021.127007

Zhang T, Su X, Zhang G, et al (2022a) Evaluation of the impacts of human activities on propagation from meteorological drought to hydrological drought in the Weihe River Basin, China. Sci Total Environ 819:. https://doi.org/10.1016/j.scitotenv.2022.153030

Zhang X, Hao Z, Singh VP, et al (2022b) Drought propagation under global warming: Characteristics, approaches, processes, and controlling factors. Sci Total Environ 838:156021

Zhou J, Li Q, Wang L, et al (2019) Impact of climate change and land-use on the propagation from meteorological drought to hydrological drought in the eastern Qilian Mountains. Water 11:1602

Zhou K, Li J, Zhang T, Kang A (2021) The use of combined soil moisture data to characterize agricultural drought conditions and the relationship among different drought types in China. Agric Water Manag 243:106479

Zhu Y, Liu Y, Wang W, et al (2021) A global perspective on the probability of propagation of drought: From meteorological to soil moisture. J Hydrol 603:126907

Statements and Declarations

Ethical Approval: "Not applicable."

Consent to Participate: The research data were not prepared through a questionnaire.

Consent to Publish: There is no conflict of interest regarding the publication of this article.

Authors Contributions: All authors contributed to the study conception and design. Material preparation, data collection and analysis were performed by Mehdi Mohammadi Ghaleni and Saeed Sharafi. The first draft of the manuscript was written by Mahmood Sadat-Noori and all authors commented on previous versions of the manuscript. All authors read and approved the final manuscript.

Funding: No funding was received to assist with the preparation of this manuscript.

Competing Interests: The authors have no competing interests to declare that are relevant to the content of this article.

Data availability statement: The authors affirm that the data supporting the findings of this study are included in the paper. If raw data files in another format are required, they can be obtained from the corresponding author upon reasonable request.